

# Winter Model at Finite Volume

U. G. Aglietti

*Dipartimento di Fisica, Università di Roma “La Sapienza”*

## Abstract

We study Winter or  $\delta$ -shell model at finite volume (length), describing a small resonating cavity weakly-coupled to a large one. For generic values of the coupling, a resonance of the usual model corresponds, in the finite-volume case, to a compression of the spectral lines; For specific values of the coupling, a resonance corresponds instead to a degenerate or quasi-degenerate doublet. Secular terms occur in the perturbative expansion of the spectrum from third order in the coupling on, which are resummed by means of standard multi-scale methods. The resulting improved perturbative expansions provide a rather complete analytic description of resonance dynamics at finite volume.

# 1 Introduction

Resonances occur in quantum mechanics when a discrete state is immersed and weakly-coupled to a continuum [1, 2, 3, 4, 5]. When expressed as superposition of energy eigenstates of the real (interacting) system, a resonance is represented by a narrow wave packet and is therefore a quasi-stationary state — a kind of unstable state.

It is interesting, at the fundamental level, to see what happens to a resonant state, if the continuum of its decay products is replaced by a set of closely-spaced discrete levels. This problem is also of interest in lattice field theory, where finite-size effects are currently used to determine scattering quantities [6, 7, 8, 9, 10]. We study this general problem in a specific case, the so-called Winter or  $\delta$ -shell model [11, 12, 13, 14, 15, 16, 17, 18, 19]. Once formulated on a segment of the real line, this model describes a small resonating cavity weakly-coupled to a large one; The resonant states of the small cavity are coupled to close, equally-spaced momentum levels.

The Hamiltonian of Winter model reads, in proper units [13],

$$\hat{H} = -\frac{\partial^2}{\partial x^2} + \frac{1}{\pi g} \delta(x - \pi); \quad (1)$$

where  $g \neq 0$  is a coupling constant. In the usual case, the particle coordinate  $x$  is restricted to the positive axis,

$$0 \leq x < \infty \quad (2)$$

and its wavefunction vanishes at the origin:

$$\psi(x = 0; t) = 0; \quad t \in \mathbb{R}. \quad (3)$$

We generalize the model by restricting the particle to a segment,

$$0 \leq x \leq L < \infty, \quad (4)$$

and assuming a vanishing (or reflecting) boundary condition also at the final endpoint of the segment:

$$\psi(x = L; t) = 0; \quad t \in \mathbb{R}. \quad (5)$$

Winter model at infinite volume is recovered from the finite-volume one by taking the limit  $L \rightarrow +\infty$ . Let us remark that usual Winter model is a one-parameter model — namely the coupling  $g$  — while its extension at finite volume is a two-parameter model — namely  $g$  and  $N$ . Even after the extension to finite volume, the model remains relatively simple, so that computations can still be made, to some extent, analytically.

## 2 Spectrum

By squeezing the system, the continuous spectrum of usual Winter model turns into a discrete one, with eigenfunctions

$$\psi_k(x) = \mathcal{N}_k \left\{ \theta(\pi - x) \sin(\pi N k) \sin(kx) + \theta(x - \pi) \sin(\pi k) \sin[k(L - x)] \right\}; \quad (6)$$

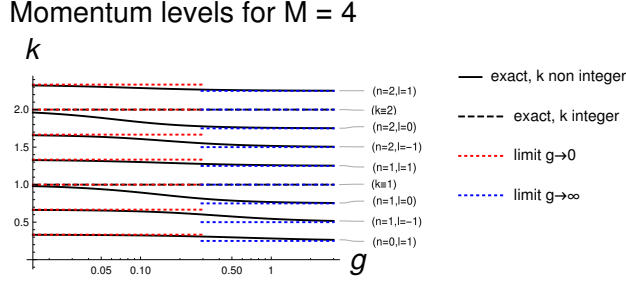


Figure 1: First nine momentum levels  $k$  as functions of the coupling  $g$ , namely  $k = k(g)$  (black continuous and dashed lines), of Winter model at  $M = 4$ , i.e. for the system with the large cavity three times bigger than the small one. The red dotted lines represent the free limit of the levels ( $\lim_{g \rightarrow 0} k(g)$ ), while the blue dotted lines represent the strong-coupling limit ( $\lim_{g \rightarrow \infty} k(g)$ ). The degeneracy for  $g \rightarrow 0$  of the flat level  $k \equiv 1$  (the lower black dashed line) with the resonating level right below it — in an otherwise equally-spaced spectrum — is clearly visible (the latter is the level  $k_1(g)$ : see text); A similar degeneracy occurs between the level  $k \equiv 2$  (the upper black dashed line) and the level right below it (the level  $k_2(g)$ ). The level spacing in the free limit,  $\Delta k_{g=0} = 1/(M - 1) \simeq 0.33$ , is given by the distance between two adjacent red lines, while the spacing in the strong-coupling limit,  $\Delta k_{g=\infty} = 1/M = 0.25$ , is given by the distance between two adjacent blue lines. The fact that the free-theory spacing is larger than the strong-coupling one is clearly visible. Note that the horizontal scale (that of the coupling  $g$ ) is logarithmic.

where  $\theta(z) \equiv 1$  for  $z > 0$  and zero otherwise is the Heaviside unit step function and the parameter  $N > 0$  is defined by the relation

$$L = (N + 1)\pi. \quad (7)$$

$N$  is therefore the length, divided by  $\pi$ , of the segment  $(\pi, L)$ , i.e. the length of the large cavity to which the small cavity  $(0, \pi)$  is coupled. The normalization constant has the explicit expression:

$$\mathcal{N}_k \equiv \left\{ \sin^2(\pi N k) \left[ \frac{\pi}{2} - \frac{\sin(2\pi k)}{4k} \right] + \sin^2(\pi k) \left[ \frac{\pi N}{2} - \frac{\sin(2\pi N k)}{4k} \right] \right\}^{-1/2}. \quad (8)$$

The quantum number  $k > 0$  is a non-integer momentum, satisfying the real transcendental equation

$$\cot(\pi k) + \cot(\pi N k) + \frac{1}{\pi g k} = 0. \quad (9)$$

Let us assume for simplicity's sake that  $N$  is an integer; That is to say that the length of the large cavity is an exact multiple of the length of the small one. For integer

$$k = n = 1, 2, 3, \dots, \quad (10)$$

there are the additional  $C^\infty(0, L)$  eigenfunctions, exactly vanishing at  $x = \pi$ ,

$$\varphi_n(x) = \sqrt{\frac{2}{L}} \sin(nx). \quad (11)$$

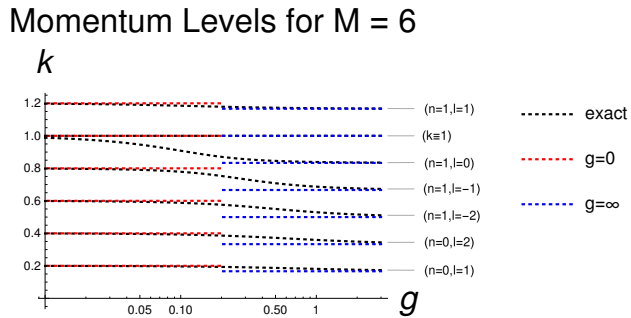


Figure 2: *Lowest seven momentum levels, containing the first resonance, of Winter model for  $M = 6$ . The black dotted lines represent the exact levels, the red dotted lines the free limit  $g \rightarrow 0$  and the blue dotted lines the strong-coupling limit  $g \rightarrow \infty$ . The degeneracy for  $g \rightarrow 0$  of the flat level  $k \equiv 1$  with the level just below it, namely the resonant level  $k_1(g)$ , is clearly visible. One may also notice that the level spacing at  $g = 0$ , given by  $\Delta k_{g=0} = 1/(M - 1) = 0.2$ , is larger than the spacing at  $g = \infty$ , which is equal to  $\Delta k_{g=\infty} = 1/M \simeq 0.167$ . Also in this case, the horizontal scale is logarithmic.*

## 2.1 Strong-coupling limit

For  $g \rightarrow +\infty$ , i.e. in the strong-coupling limit, eq.(9) basically simplifies into the elementary equation

$$\sin(\pi M k) = 0; \quad (12)$$

where

$$M \equiv N + 1 \quad (13)$$

is the total length of the system (small cavity + large cavity) in units of  $\pi$ . The solutions of the above equation are the momenta (see figs.1, 2 and 3)

$$k = \frac{s}{M}, \quad s = 1, 2, 3, \dots \quad (14)$$

When  $s$  is an integer multiple of  $M$ , then the above momentum is integer:

$$s = n M \Rightarrow k = n; \quad n = 1, 2, 3, \dots \quad (15)$$

For  $g \rightarrow \infty$ , the potential barrier, given by the  $\delta$ -function, completely disappears and the system reduces to a free particle in the box  $[0, L]$ . The level spacing in this limit has the constant value

$$\Delta k_{g=\infty} = \frac{1}{N + 1}. \quad (16)$$

Therefore, in the strong-coupling limit, the momentum spectrum of finite-volume Winter model goes into a non-degenerate, equally-spaced spectrum.

## 2.2 Free limit

For  $g \rightarrow 0^+$ , i.e. in the free limit, according to eq.(9), the allowed momenta are of the form (see figs. 1, 2 and 3)

$$k = \frac{s}{N}. \quad (17)$$

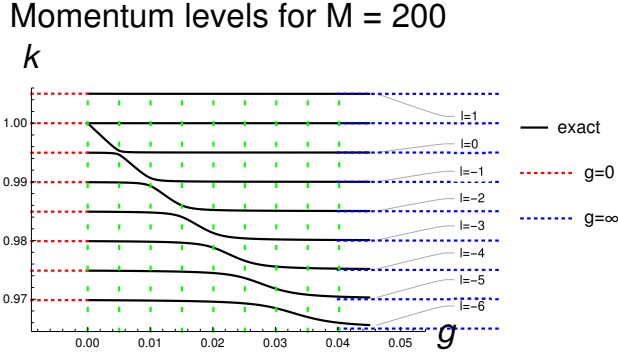


Figure 3: *Momentum levels around the first or fundamental resonance ( $n = 1$ ) for volume  $M = 200$ . The black continuous lines represent the exact levels, the red dotted lines the free limit  $g \rightarrow 0$  and the blue dotted lines the strong-coupling limit  $g \rightarrow \infty$ . The vertical light green dashed lines at  $g = j/199 \cong 0.005 \times j$  ( $j = 0, 1, 2, 3, \dots$ ) represent the coupling values where exactly-degenerate doublets ( $j = 0$ ) or quasi-degenerate doublets ( $j > 0$ ) occur in the spectrum.*

When  $s$  is an integer multiple of  $N$ , then the momentum in the above equation is integer:

$$s = nN \quad \Rightarrow \quad k = n; \quad n = 1, 2, 3, \dots \quad (18)$$

In general, by means of the euclidean division of  $s$  by  $N$ ,

$$s = nN + l, \quad (19)$$

the free-theory momentum can be written

$$k = n + \frac{l}{N}. \quad (20)$$

It is natural to take the remainder  $l$  in the (quasi-)symmetric range

$$-\frac{N}{2} < l \leq \frac{N}{2}. \quad (21)$$

In the following, a momentum level  $k$  considered as a function of the coupling  $g$ ,  $k = k(g)$ , which is equal to  $n + l/N$  in the limit  $g \rightarrow 0$ , will be called a  $(n, l)$  level or more simply a  $l$  level.

In the free limit, the potential barrier at  $x = \pi$  becomes impermeable, so that the system decomposes into two non-interacting subsystems: a free particle in the small box  $[0, \pi]$  and a free particle in the large box  $[\pi, M\pi]$ . The level spacing in the free limit is given by:

$$\Delta k_{g=0} = \frac{1}{N}. \quad (22)$$

Note that it is larger than the strong-coupling spacing (cfr. eq.(16)). When  $s$  is an integer multiple of  $N$ ,

$$s = nN, \quad n = 1, 2, 3, \dots, \quad (23)$$

then the free-theory momentum in eq.(17) is integer:

$$k = n. \quad (24)$$

Since wavefunctions with integer momenta are eigenfunctions of both the small cavity and the large one, such states have a double degeneracy. In physical terms, the particle can be entirely and permanently confined either in the small cavity or in the large one. This double degeneracy "compensates" for the larger  $g \rightarrow 0$  spacing, giving rise to the same average level density as for  $g \rightarrow \infty$ . To summarize, in the free limit, the momentum spectrum of finite-volume Winter model goes into an equally-spaced spectrum, eq.(17), with a double degeneracy at integer momenta, eq.(24).

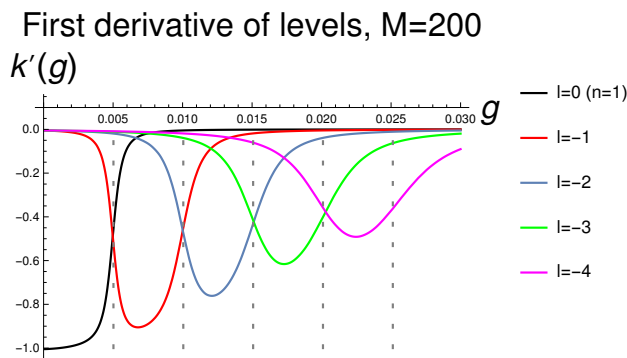


Figure 4: *First derivatives of momentum levels as functions of the coupling, namely  $k'(g)$ , below and including the first or fundamental resonance ( $n = 1$ ) for  $M = 200$ . The vertical gray dashed lines at  $g = j/199 \cong 0.005 \times j$  ( $j = 1, 2, 3, \dots$ ) represent the coupling values where quasi-degenerate doublets occur in the spectrum. Note that the regions around the minima of  $k'(g)$  lie between two consecutive dashed lines.*

## 2.3 Discussion

In figs. 1 and 2, we plot the lowest momentum levels  $k$  as functions of the coupling  $g$ , namely  $k = k(g)$ , of Winter model in the small-volume cases  $M = 4$  and  $M = 6$  respectively. The curves are obtained through numerical solution of eq.(9), determining, apart from the "exceptional" levels  $k \equiv n = 1, 2, 3, \dots$ , the complete momentum spectrum of the model. After excluding the flat levels, corresponding to the eigenfunctions in eq.(11), we observe that each momentum level is a strictly monotonically-decreasing function of  $g$ , with an upper horizontal asymptote given by the free limit ( $g \rightarrow 0$ ), represented by a dotted red line, and a lower horizontal asymptote given by the strong-coupling limit ( $g \rightarrow \infty$ ), represented by a dotted blue line. By approaching a flat level from below, one hits levels with total variation (the distance between the red line and the lower blue line) progressively bigger; The total variation of the level right above a flat one is instead extremely small. Therefore, a flat level separates the levels having a resonant behavior (below it) from the levels not having such a behavior (above it). A degeneracy for  $g \rightarrow 0$  of the level  $k \equiv 1$  with the level right below it (whose physical origin has been explained in sec. 2.2 ) is clearly

seen in both figs. 1 and 2; A similar degeneracy of the level  $k \equiv 2$  with the level right below it is also visible in fig. 2.

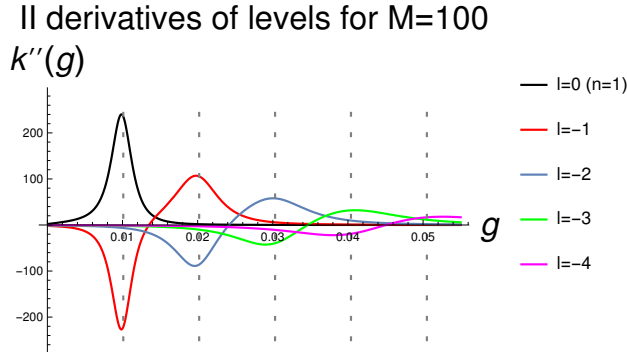


Figure 5: *Second derivatives of momentum levels as functions of the coupling,  $k''(g)$ , below and including the first or fundamental resonance ( $n = 1$ ) for  $M = 200$ . We observe that the maxima and the minima of the second derivatives of the levels are pretty close to the gray vertical dashed lines.*

In fig. 3, we plot the momentum levels around the first or fundamental resonance  $n = 1$  ( $l = 0$ ) in the large-volume case  $M = 200$ . We see that the resonant level  $l = 0$  (the level right below the constant one  $k \equiv 1$ ) goes down roughly in a linear way with the coupling, from the free point  $g = 0$  (where it is degenerate with  $k \equiv 1$ , as we have already seen in the small- $M$  cases above) up to  $g \approx g_1 \equiv 1/N \cong 0.005$ , where it shows a sharp variation of its first derivative — a quick increase up to zero (see figs. 4 and 5). For  $g \gtrsim g_1$ , this level is roughly constant, having already basically reached its infinite-coupling limit.

In general, the levels with  $l < 0$  (below the resonant one) are pretty flat for very small and very large couplings and show a sharp transition at  $g = \mathcal{O}(1/N)$ , when they substantially go from their free values down to their infinite-coupling values. To be more specific, the  $l = -1$  level, for example, is basically constant from  $g = 0$  up to  $g \approx g_1$ , where it shows a sharp decrease of its first derivative. Then, in the coupling interval

$$g_1 \lesssim g \lesssim g_2 \equiv \frac{2}{N} \cong 0.01, \quad (25)$$

this level goes down linearly with  $g$ . At  $g \approx g_2$ , it shows a sharp increase of its first derivative up to zero and finally, for  $g \gtrsim g_2$ , it is roughly constant, having basically reached its infinite-coupling limit. In general, the non-resonant level of index  $l = -1, -2, -3, \dots$  is constant from  $g = 0$  up to roughly  $g_{|l|} \equiv |l|/N \cong 0.005 \times |l|$ , where it shows a sharp decrease of its first derivative. In the coupling interval

$$g_{|l|} \lesssim g \lesssim g_{|l|+1} \cong 0.005 \times (|l| + 1), \quad (26)$$

the level goes down roughly linearly with  $g$ . For  $g \approx g_{|l|+1}$ , it shows a sharp increase of its first derivative up to zero and above this point it is basically flat. By getting far from the resonance level, i.e. by increasing  $|l|$ , the above behavior is softened. Since the transition

regions of different  $l$  levels are shifted, for values of the coupling

$$g \approx g_j \equiv \frac{j}{N} \cong 5 \times 10^{-3} \times j; \quad j = 1, 2, 3, \dots; \quad (27)$$

corresponding to the vertical dashed green lines in fig. 3, two black curves almost get in touch with each other, implying that the corresponding doublet is quasi degenerate (see fig. 6). For the exceptional values of the coupling  $g = g_j$  in eq.(27), the first resonance ( $n = 1$ ) of the infinite-volume model corresponds to the quasi-degenerate doublet having momenta, in the free limit  $g \rightarrow 0$ , given by  $1 - (j - 1)/N$  and  $1 - j/N$ . The distance between the quasi-degenerate levels rapidly grows with  $j$ , so that this approximate degeneracy is barely visible for, let's say,  $j = \mathcal{O}(5)$ .

Between the first two vertical green dashed lines (see fig. 3), i.e. in the coupling range

$$0 \lesssim g \lesssim g_1, \quad (28)$$

there are *three* levels — rather than *two* as in general — in the momentum interval

$$0.995 \lesssim k \lesssim 1, \quad (29)$$

of width

$$\Delta k \simeq 5 \times 10^{-3} \simeq \frac{1}{N} \simeq \frac{1}{N+1}; \quad (N = 199 \gg 1). \quad (30)$$

So long as  $j = 1, 2, 3, \dots$  is not too large, this "compression" of three levels also occurs in the coupling intervals

$$g_j \cong 5 \times 10^{-3} j \lesssim g \lesssim g_{j+1} \cong 5 \times 10^{-3} (j + 1). \quad (31)$$

For large  $j$ , i.e. for large values of the coupling  $g$  compared to  $1/N$ , a resonance corresponds to a mild compression of many momentum lines.

We may summarize the above findings by saying that, for the exceptional values of the coupling  $g = g_j \equiv j/N$ , eq.(27), the fundamental resonance of usual Winter model corresponds, in the finite-volume case, to a quasi-degenerate doublet (see fig. 6). For generic values of the coupling, the resonance corresponds instead to a compression of three lines in the typical spacing between two of them

$$\Delta k \approx \frac{1}{N} \approx \frac{1}{N+1}; \quad (32)$$

For larger values of the coupling, i.e. for large  $j$ , the resonance corresponds to a mild compression of many levels. As in the small-volume cases considered above, only the levels below the flat one  $k \equiv 1$  exhibit a resonant behavior; The levels above it (we have plotted just one of them in fig. 3) do not "see" the resonance and are approximately constant in  $g$ .

### 3 Ordinary Perturbation Theory

In the analytic calculations, we always assume

$$0 < g \ll 1, \quad (33)$$

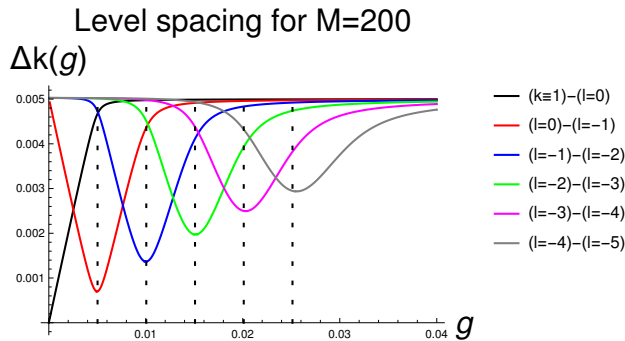


Figure 6: Level spacing  $\Delta k$  as function of the coupling  $g$ , namely  $\Delta k = \Delta k(g)$ , between the first few levels below and including the first or fundamental resonance ( $n = 1$ ) for  $M = 200$ . It is observed that the minima of the level spacing occur at  $g \approx g_j \cong 0.005 \times j$ ,  $j = 0, 1, 2, 3, \dots$ , pretty close to the vertical gray dashed lines. By increasing  $j$ , the minima get less pronounced.

i.e. a weakly-repulsive interaction, in order to use perturbation theory in  $g$  and avoid bound-state effects [13]. The momentum on the r.h.s. of eq.(17) can be considered the zero order term of a perturbative expansion in the coupling  $g$ . One has to distinguish between:

1. *Resonant case*, when  $s$  is an integer multiple of  $N$ ,

$$s = nN; \quad n = 1, 2, 3, \dots, \quad (34)$$

so that the unperturbed momentum is integer,

$$k = n; \quad (35)$$

2. *Non-resonant case*, when  $s$  is not multiple of  $N$ , i.e. the fraction on the r.h.s. of eq.(17) is not apparent. The unperturbed momentum is written in this case

$$k = n + \frac{l}{N}; \quad (36)$$

with

$$-\frac{N}{2} < l \leq \frac{N}{2}; \quad l \neq 0. \quad (37)$$

The perturbation expansion of the constant levels  $k \equiv n$  is of course trivial, as these levels do not depend on  $g$ .

### 3.1 Resonant case

In the resonant case, the expansion is written

$$k_n = k_n(g) = n \left( 1 + \sum_{i=1}^{\infty} g^i c_n^{(i)} \right); \quad n = 1, 2, 3, \dots; \quad (38)$$

Note that we label the momentum levels by means of their limiting values for  $g \rightarrow 0$ :

$$k_n(g=0) = n. \quad (39)$$

By recursively solving in  $g$  the momentum eigenvalue eq.(9), one obtains for the first few coefficients:

$$c_n^{(1)} = - \left( 1 + \frac{1}{N} \right); \quad (40)$$

$$c_n^{(2)} = + \left( 1 + \frac{1}{N} \right)^2;$$

$$c_n^{(3)} = + \left( 1 + \frac{1}{N} \right)^3 \left( \frac{\pi^2}{3} n^2 N - 1 \right). \quad (41)$$

The resonances of the usual, infinite-volume model are related to the poles in the complex  $k$ -plane [12, 13]

$$k = \chi_n(g) = n \left( 1 + g b_n^{(1)} + g^2 b_n^{(2)} + \dots \right), \quad (42)$$

where

$$b_n^{(1)} = -1; \quad b_n^{(2)} = +1 - i\pi n. \quad (43)$$

For  $N \rightarrow \infty$ , i.e. in the infinite-volume limit, the first-order coefficient  $c_n^{(1)}$  smoothly goes into the corresponding coefficient  $b_n^{(1)}$  of the infinite-volume theory; furthermore,  $c_n^{(2)}$  goes into the real part of  $b_n^{(2)}$ . Surprises come at third order: By looking at the expression of the third-order coefficient  $c_n^{(3)}$  above, we find a secular term proportional to  $N$ , giving a contribution to  $k_n$  of the form  $g^3 N$ . By analyzing higher-order coefficients (which we have not displayed), we find that the occurrence of positive powers of  $N$  is a general phenomenon: The term  $g^i c_n^{(i)}$ ,  $i = 3, 4, 5, \dots$ , contains monomials of the form

$$g^2 (gN)^{i-2}, \quad g^3 (gN)^{i-3}, \quad g^4 (gN)^{i-4}, \quad \dots \quad (44)$$

Therefore we have to restrict the range of the perturbative expansion to the parameter-space region

$$0 < gN \ll 1, \quad \text{or equivalently} \quad 0 < g \ll \frac{1}{N}. \quad (45)$$

For small sizes of the large cavity, let's say  $N = \mathcal{O}(1)$ , the secular terms in (44) do not present any problem, as they do not lead to any substantial enhancement in the coefficients  $c_n^{(i)} = c_n^{(i)}(N)$  entering the expansion of  $k_n = k_n(g, N)$ . For large  $N$ , the terms in (44) tend instead to spoil the perturbative expansion. The occurrence of secular terms in the momentum expansion implies in particular that we can no more take the infinite-volume limit in a straightforward way, as we have made in the first-order and second-order cases.

In the very small coupling region (45), the allowed momentum

$$k_n(g) = n - gn \left( 1 + \frac{1}{N} \right) + \dots \quad (46)$$

is very close to — slightly below — the exactly-integer momentum

$$\bar{k}_n \equiv n, \quad (47)$$

whose eigenfunction has been given in eq.(11). Their separation vanishes indeed in the free limit:

$$\bar{k}_n - k_n(g) = g n \left(1 + \frac{1}{N}\right) + \dots . \quad (48)$$

The conclusion is that for very small couplings,  $g \ll 1/N$ , the quasi-degenerate doublet

$$\left(k_n(g), \bar{k}_n\right) \quad (49)$$

corresponds to the  $n^{\text{th}}$  resonance of the usual, infinite-volume model, for any  $n = 1, 2, 3, \dots$ . Ordinary perturbation theory therefore allows an analytic description of the exact double degeneracy for  $g \rightarrow 0$ , which we have observed in the plots of the exact levels in figs. 1, 2, 3 and 6.

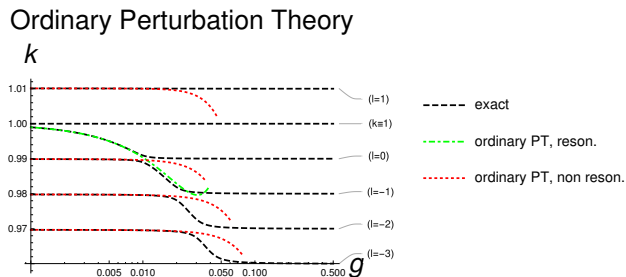


Figure 7: *Momentum levels around the first or fundamental resonance ( $n = 1$ ) as functions of the coupling,  $k = k(g)$ , for the case  $M = 100$ . The black dashed lines are the plots of the exact levels, the green dot-dashed line represents the ordinary perturbative formula for the resonant case ( $l = 0$ ), while the red lines are the plots of the perturbative formulae in the non-resonant cases ( $l \neq 0$ ). The horizontal scale is logarithmic.*

### 3.2 Non-resonant case

In the non-resonant case, the perturbative expansion, according to eq.(36), is written:

$$k = k_{n+l/N}(g) = \left(n + \frac{l}{N}\right) \left(1 + \sum_{i=1}^{\infty} g^i c_{n+l/N}^{(i)}\right). \quad (50)$$

As in the resonant case, the momentum levels, as functions of the coupling, are labeled by their limiting values for  $g \rightarrow 0$ :

$$k_{n+l/N}(g = 0) = n + \frac{l}{N}. \quad (51)$$

The lowest-order coefficients of the perturbative expansion have the following explicit expressions:

$$c_{n+l/N}^{(1)} = -\frac{1}{N}; \quad (52)$$

$$c_{n+l/N}^{(2)} = +\frac{\pi}{N} \left( n + \frac{l}{N} \right) \cot \left( \frac{\pi l}{N} \right) + \frac{1}{N^2};$$

$$c_{n+l/N}^{(3)} = -\frac{\pi^2}{N} \left( 1 - \frac{1}{N} \right) \left( n + \frac{l}{N} \right)^2 \operatorname{csc}^2 \left( \frac{\pi l}{N} \right) +$$

$$-\frac{3\pi}{N^2} \left( n + \frac{l}{N} \right) \cot \left( \frac{\pi l}{N} \right) + \frac{4\pi^2}{3N} \left( n + \frac{l}{N} \right)^2 - \frac{1}{N^3}; \quad (53)$$

where  $\cot(x)$  and  $\operatorname{csc}(x)$  are the cotangent and the cosecant of  $x$  respectively. By expanding the above coefficients for large  $N$ , one obtains:

$$c_{n+l/N}^{(1)} = -\frac{1}{N};$$

$$c_{n+l/N}^{(2)} = +\frac{n}{l} + \frac{1}{N} + \mathcal{O} \left( \frac{1}{N^2} \right);$$

$$c_{n+l/N}^{(3)} = -\left( \frac{n}{l} \right)^2 N + \frac{n(n-2l)}{l^2} + \frac{\pi^2 n^2 - n/l - 1}{N} + \mathcal{O} \left( \frac{1}{N^2} \right). \quad (54)$$

In general, any additional power of the coupling  $g$  brings, inside its corresponding coefficient, an additional power of  $N$ ; The third-order coefficient, in particular, has a secular term linear in  $N$ , as in the resonant case.

### 3.3 Discussion

In fig. 7 we plot the exact momentum levels around the first resonance ( $n = 1$ ) together with their ordinary perturbative expansions, for  $M = 100$ . The green dot-dashed curve, representing the perturbative expansion of the first resonant level (the plot of eq.(38) with  $n = 1$  truncated at third order in  $g$ ) is very close to the corresponding exact curve (the black dashed line) from  $g = 0$  up to  $g \approx 10^{-2}$ ; Around this point (as already seen in the  $M = 200$  case), the exact curve basically reaches its lower asymptote, showing a quick and large variation of its first derivative and getting pretty close to the lower, non-resonating, curve  $l = -1$ . For values of the coupling in the region

$$10^{-2} \lesssim g \lesssim 2 \times 10^{-2}, \quad (55)$$

the resonant perturbative curve is rather close to (a little above actually) the exact curve of the non-resonant level  $l = -1$ . Above  $g \approx 2 \times 10^{-2}$ , the perturbative curve shows an unphysical rise and is no more able to describe any level. It is noticeable that a single perturbative formula describes *two* distinct levels — rather than one — in two different coupling regions.

The graphs of the perturbative expansions of the non-resonant levels for  $l < 0$  (the red dotted lines below the green dot-dashed line) remain close to the corresponding exact

curves (black dashed lines) from  $g = 0$  up to the coupling region where the latter make a transition from the upper asymptote to the lower one. The perturbative curves are not able to correctly reproduce this transition, showing some sort of "delay". As in previous fig. 3, the exact curve of the non-resonant level  $l = 1$  (the level right above  $k \equiv 1$ ) is pretty flat in all the coupling range; The corresponding perturbative curve (the red dotted line above the green dot-dashed line) is close to the exact one from  $g = 0$  up to approximately  $g \approx 2 \times 10^{-2}$ , where it shows an unphysical decrease.

## 4 Resummed Perturbation Theory

The parameter-space region

$$gN \gtrsim 1, \quad (56)$$

which is out of control with ordinary perturbation theory as we have seen in the previous section, can be studied by means of improved perturbative expansions, generated in the limit

$$g \rightarrow 0^+, \quad N \rightarrow +\infty \quad \text{with} \quad \xi \equiv gN \rightarrow \text{constant}. \quad (57)$$

As in the case of ordinary perturbation theory, we have to treat separately the resonant momenta and the non-resonant ones.

### 4.1 Resonant case

In the resonant case, the  $k_n$ 's are represented by function series of the form:

$$k_n = n \left( 1 + \sum_{i=1}^{\infty} g^i h_n^{(i)}(\xi) \right). \quad (58)$$

By means of standard multi-scale techniques [20], one obtains for the lowest-order functions:

$$\begin{aligned} h_n^{(1)}(\xi) &= -1; \\ h_n^{(2)}(\xi) &= -\nu \cot(\nu\xi) + 1; \\ h_n^{(3)}(\xi) &= +\nu^3 \xi \cot^3(\nu\xi) - \nu^2(1+\xi) \cot^2(\nu\xi) + \\ &\quad + \nu(\nu^2\xi + 3) \cot(\nu\xi) + \nu^2 \left( \frac{1}{3} - \xi \right) - 1; \end{aligned} \quad (59)$$

where we have defined

$$\nu \equiv \pi n. \quad (60)$$

The functions  $g^i h_n^{(i)}(\xi)$ ,  $i > 1$ , have pole singularities whenever

$$nNg = j = 1, 2, 3, \dots. \quad (61)$$

For a given size of the large cavity, i.e. for given  $N$ , and for a given resonance, i.e. for given  $n$ , the functions  $h_n^{(i)}(\xi)$  become singular when the coupling  $g$  approaches one point of the sequence

$$g_j \equiv \frac{j}{nN}; \quad j = 1, 2, 3, \dots. \quad (62)$$

As we have seen in figs. 3–6, the points  $g_j$  are the particular values of the coupling  $g$  where the exact levels present a large variation of their first derivatives and quasi-degenerate doublets occur in the spectrum.

A physical argument about the origin of the above singularities is the following. The eigenfunctions of a free particle in the box  $(0, \pi)$  have exactly integer momenta:

$$k_{\text{box}(0,\pi)} = n; \quad n = 1, 2, 3, \dots \quad (63)$$

By weakly-coupling such states to a continuum, the box becomes a resonating cavity and the above momenta are subjected to a finite renormalization [13, 14], which, to first order in  $g$ , gives

$$\chi_n(g) \approx n - ng. \quad (64)$$

Now, if we couple the box  $(0, \pi)$  to a large box  $(\pi, L)$  — rather than to the half line  $(\pi, \infty)$  —, we expect singularities to occur in the perturbative expansion of  $k_n = k_n(g, \xi)$ , when a resonant momentum  $\chi_n(g)$  of the infinite-volume theory becomes equal to an allowed momentum of the particle in the large box, namely

$$\chi_n(g) \approx n + \frac{l}{N}. \quad (65)$$

By replacing the explicit form of  $\chi_n(g)$ , we obtain the relation

$$nNg \approx -l. \quad (66)$$

If we now identify  $j$  with  $-l$ , we obtain eq.(61).

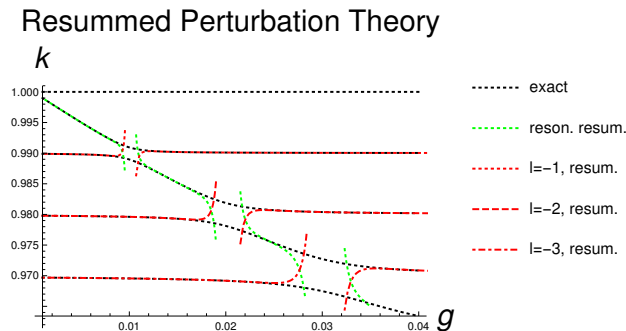


Figure 8: *Few momentum levels below the first or fundamental resonance ( $n = 1$ ) for  $M = 100$ . The black dotted lines are the plots of the exact levels, the green dotted line represents the resummed formula in the resonant case ( $l = 0$ ), while the red lines represent the resummed formulae in the non-resonant cases ( $l \neq 0$ ). To be more specific, the red dotted line is the level  $l = -1$ , the red dashed line is the level  $l = -2$  and the red dot-dashed line is the level  $l = -3$ . The singularities of the resummed formulae at the points  $g = g_j \equiv j/(nN) = j/99 \cong 0.01 \times j$ , corresponding to quasi-degenerate doublets and large variations of their first derivatives, are clearly visible for  $j = 1, 2, 3$ .*

## 4.2 Non-resonant case

In the non-resonant case, the resummed expansion in the effective coupling  $\xi$  for the quantized momentum  $k_{n+l/N} = k_{n+l/N}(g, \xi)$  is written:

$$k_{n+l/N} = \left( n + \frac{l}{N} \right) \left( 1 + \sum_{i=2}^{\infty} g^i h_{n+l/N}^{(i)}(\xi) \right); \quad (67)$$

where:

$$\begin{aligned} h_{n+l/N}^{(2)}(\xi) &= \frac{n}{l+n\xi} - \frac{1}{\xi}; \\ h_{n+l/N}^{(3)}(\xi) &= \frac{ln^2}{(l+n\xi)^3} - \frac{ln}{(l+n\xi)^2} - \frac{n}{l+n\xi} + \frac{1}{\xi}. \end{aligned} \quad (68)$$

The series begins at second order in  $g$  because the term

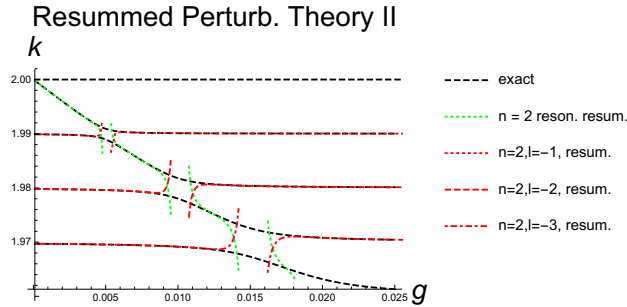


Figure 9: *Few momentum levels below the second or first-excited resonance ( $n = 2$ ) for the case  $M = 100$ . The plot scheme is the same as in previous figure 8, so we do not repeat its description. The singularities of the resummed formulae at  $g = j/198 \simeq 0.005 \times j$ , corresponding to quasi-degenerate doublets and large variations of their first derivative, are clearly visible for  $j = 1, 2, 3$ .*

$$\frac{l}{N} = \frac{gl}{\xi} \quad (69)$$

is already of first order and the perturbative expansion is supposed to be a small correction to the unperturbed result.

The momentum  $k_{n+l/N}$ , as given by the r.h.s. of eq.(67) truncated at some order in  $g$ , is approximated by a sum of rational functions of the coupling  $g$ , i.e. by a rational function of  $g$ , rather than by a polynomial in  $g$ , as in ordinary perturbation theory.

For a given size of the large cavity, i.e. for given  $N$ , and for a given state, i.e. for given  $n$  and  $l$ , the functions  $h_{n+l/N}^{(i)}$ , describing the levels close to the  $n^{\text{th}}$  resonance, become singular when the coupling  $g$  approaches the value

$$g = g_{-l} \equiv \frac{-l}{nN}; \quad l = \pm 1, \pm 2, \pm 3, \dots \quad (70)$$

In the repulsive case to which we restrict,  $g > 0$ , the above singularity occurs for  $l < 0$  only, i.e. in the levels below the resonant one.

### 4.3 Discussion

In fig. 8 we compare the exact momentum levels below and including the first resonance  $n = 1$  (black dotted lines), with the corresponding resummed (perturbative) expansions (green dotted line and red lines). Let's first discuss the simpler non-resonant case. The resummed formula for the  $l^{\text{th}}$  level given in eq.(67) (the red dotted, dashed and dot-dashed line for  $l = -1, -2$  and  $-3$  respectively) correctly reproduces the corresponding  $l^{\text{th}}$  level from  $g = 0$  almost up to its singularity, at

$$g_{|l|} = \frac{|l|}{99} \cong 0.01 \times |l|. \quad (71)$$

For example, the  $l = -1$  resummed formula (the red dotted line) describes pretty well this level from  $g = 0$  almost up to its singularity, at  $g_1 \cong 0.01$ . But what happens for larger, still perturbative, couplings? The problem is that the resummed formula in eq.(67) is *not continuous* at  $g = g_{|l|}$ , because of its pole singularity at this point. It is therefore not clear *a priori* which level this formula is going to describe beyond this singularity, if any. In particular, there is no reason to expect that this formula will still describe the  $l^{\text{th}}$  level after the singularity, i.e. for  $g > g_{|l|}$ . By looking at fig. 8, it is found that for couplings slightly above  $g_{|l|}$  up to relatively large values of  $g$ , the  $l^{\text{th}}$  resummed curve reproduces quite accurately the next upper level, i.e. the level with index  $l + 1$ . For example, if we fix the value  $l = -1$  in eq.(67), we obtain a formula which reproduces the exact curve  $l = -1$  below the singularity at  $g = g_1 \cong 0.01$ , and the resonant level  $l = 0$  above  $g_1$ . In general, therefore, a resummed formula for a non-resonant level describes two different momentum levels, in two different coupling regions.

Let's now consider the effects of the resummation to all orders in  $\xi$  of the perturbative series for a resonant level. The (truncated) function series on the r.h.s. of eq.(58) has a sequence of pole singularities located, in the case of the first resonance  $n = 1$  and volume  $N = 99$ , at

$$g = g_j \equiv \frac{j}{nN} = \frac{j}{99} \cong 0.01 \times j; \quad j = 1, 2, 3, \dots \quad (j \ll N). \quad (72)$$

As in the non-resonant case, the resummed formula in eq.(58) does not need to describe above each singularity, i.e. for  $g > g_j$ , the same level described below it, i.e. for  $g < g_j$ . By looking at fig. 8, it is found that the resummed resonant level  $n = 1$  (the green dotted curve) reproduces pretty well, from  $g = 0$  up to almost its first singularity at  $g_1 \simeq 0.01$ , the exact first resonant level. Between the first and the second singularity, i.e. for values of the coupling in the interval

$$g_1 \simeq 0.01 \lesssim g \lesssim g_2 \simeq 0.02, \quad (73)$$

the  $n = 1$  resummed formula describes the transition region of the level right below the resonant one, i.e. the non-resonant level with  $l = -1$ . In general, in the coupling region

$$g_j \lesssim g \lesssim g_{j+1}, \quad (74)$$

the resummed formula for the fundamental resonance describes the transition region of the non-resonant level with  $l = -j$  (so long as we are in the weak-coupling regime of course). It

is remarkable that the resummed formula for the  $n^{\text{th}}$  resonance describes the  $n^{\text{th}}$  resonance level from  $g = 0$  almost up to  $g_1$ , i.e. basically its transition region, together with an entire sequence of non-resonant levels, in their respective transition regions.

In fig. 9 we compare the exact and resummed momentum levels below and including the second or first-excited resonance  $n = 2$ . In agreement with the general formula in eq.(62), the resummed formulae are singular at

$$g = g_j = \frac{j}{2N} = \frac{j}{198}; \quad j = 1, 2, 3, \dots \quad (75)$$

As we have found in fig. 8 for the first resonance (as well as in the previous  $M = 200$  plots), the exact levels exhibit at these points quasi-degenerate doublets and large variations of their first derivatives. In general, the plots for  $n = 2$  are very similar to the corresponding ones for the first resonance, so we do not repeat the discussion.

In fig. 10 we compare the momentum levels around the first resonance ( $n = 1$ ) computed with ordinary perturbation theory with the levels computed with resummed perturbation theory. In general, the resummed perturbative formulae work definitively better than the corresponding fixed-order ones. After excluding proper neighborhoods of the singularities at  $g = g_j$  ( $j = 1, 2, 3, \dots$ ) and proper matching, resummed perturbation theory correctly describes all the momentum levels so long as  $g \ll 1$ .

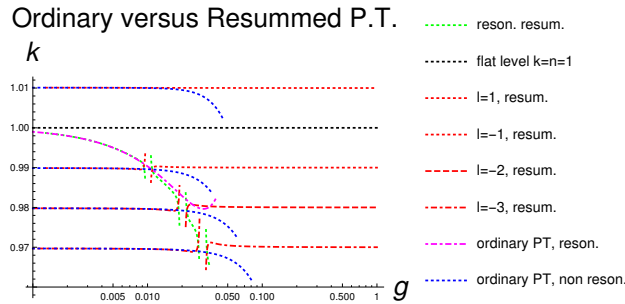


Figure 10: *Ordinary versus resummed perturbation-theory levels around the first resonance  $n = 1$ . The magenta dot-dashed curve is the plot the resonant level computed in ordinary perturbation theory, while the dotted green line describes the same level in resummed perturbation theory. The red dotted, dashed and dot-dashed curves describe the non-resonant levels in resummed perturbation theory for  $l = \pm 1$ ,  $l = -2$  and  $l = -3$  respectively, while the dotted blue lines describe the same levels in ordinary perturbation theory. The flat level  $k = \bar{k}_1 \equiv 1$  (black dotted line), separating the non-resonating levels (above it) from the resonating ones (below it), is also shown for completeness. The horizontal scale is logarithmic.*

## 5 Conclusions

We have computed the spectrum of Winter or  $\delta$ -shell model at finite volume both numerically and by means of perturbative methods. For very small repulsive couplings,

$$0 < g \ll \frac{1}{N}, \quad (76)$$

the resonance of order  $n = 1, 2, 3, \dots$  of usual Winter model corresponds, in the finite-volume case, to a quasi-degenerate doublet with momenta

$$k_n(g) = n - gn \left(1 + \frac{1}{N}\right) + \dots; \quad \text{and} \quad \bar{k}_n \equiv n. \quad (77)$$

The distance between these levels goes to zero linearly with the coupling:

$$\bar{k}_n - k_n(g) = gn \left(1 + \frac{1}{N}\right) + \dots. \quad (78)$$

The physical origin of this degeneracy is related to the fact that, for very small couplings, a wavefunction with an integer momentum is, to a good approximation, an eigenfunction of both the small cavity and the large one. In more physical terms, for  $g \rightarrow 0$ , a particle with integer momentum can be entirely and permanently confined either in the small cavity or in the large one. This degeneracy is well described by ordinary perturbation theory.

In the large-volume case,

$$N \gg 1, \quad (79)$$

new approximate degeneracies occur in the spectrum. The exact momentum levels  $k = k(g)$  show a large variation of their first derivatives and quasi-degenerate doublets occur in the spectrum when

$$g \approx g_j \equiv \frac{j}{nN}; \quad j = 1, 2, 3, \dots. \quad (80)$$

For generic values of the coupling, of the order of the inverse system size,

$$g \approx \frac{1}{N} \ll 1, \quad (81)$$

an infinite-volume resonance corresponds to the compression of three lines in the typical spacing between two of them and, by increasing further the coupling, to a mild compression of many lines, let's say  $h = 4, 5, \dots$  lines in the typical spacing of  $h - 1$  lines (see fig. 6).

The perturbative expansion of the momentum spectrum of the finite-volume model contains secular terms, from third order in  $g$  on, of the form

$$g^i N^{i-2}, \quad g^i N^{i-3}, \quad g^i N^{i-4}, \quad \dots \quad (i = 3, 4, 5, \dots). \quad (82)$$

For large volumes,  $N \gg 1$ , these terms can be of order one (or bigger) even in the weak coupling regime  $g \ll 1$ , so they tend to spoil the convergence of the perturbative series. Not surprisingly, ordinary perturbation theory is completely unable to describe these approximate degeneracy's of the spectrum. By resumming the perturbative series for the momenta to all orders in the effective coupling

$$\xi \equiv gN = \mathcal{O}(1), \quad (83)$$

one obtains improved expansions presenting pole singularities at  $g = g_j$ . We may say that, in some sense, the resummed formulae "see" the quasi-degeneracy points  $g_j$ . After the exclusion of small neighborhoods of the singular couplings  $g_j$  and proper matching of the resummed levels with the exact ones, improved perturbation theory accurately describes the

complete momentum spectrum. Let us therefore conclude by saying that resummed perturbation theory provides a satisfactory analytic description of resonances at finite volume in the case of the Winter model.

### Acknowledgments

I would like to thank M. Papinutto for discussions.

## References

- [1] G. Gamow, *Zur Quantentheorie der Atomkernes*, Z. Phys. 51, p. 204 (1928).
- [2] *Unstable states in the continuous spectra*, in Advances in Quantum Chemistry, vol.60 (2010), North Holland, edited by C. Nikolaides.
- [3] “*Unstable States in the Continuous Spectra, Part II: Interpretations, Theory and Applications*”, in Advances in Quantum Chemistry, vol.63 (2012), Elsevier, volume edited by C. A. Nicolaides and E. Brändas (Series Editors J. S. Sabin and E. Brändas ).
- [4] For resonances in quantum field theory see: L. Maiani and M. Testa, *Unstable Systems in Relativistic Quantum Field Theory*, Ann. of Phys. vol. 263, n. 2, pag. 353 (1998); F. Giacosa, *Non-exponential decay in quantum field theory and in quantum mechanics: the case of two (or more) decay channels*, Found. Phys. **42** (2012) 1262, arXiv:1110.5923 [nucl-th].
- [5] The classic references on the  $S$  matrix are: R. Newton, *Scattering of Waves and Particles*, Dover Publications, Inc. Mineola, New-York (2004); M. Goldberger and K. Watson, *Collision Theory*, Dover Publications, Inc. Mineola, New-York (2002).
- [6] M. Luscher, *Volume Dependence of the Energy Spectrum in Massive Quantum Field Theories. 1. Stable Particle States*, Commun. Math. Phys. **104** (1986) 177.
- [7] M. Luscher, *Volume Dependence of the Energy Spectrum in Massive Quantum Field Theories. 2. Scattering States*, Commun. Math. Phys. **105** (1986) 153.
- [8] M. Luscher and U. Wolff, *How to Calculate the Elastic Scattering Matrix in Two-dimensional Quantum Field Theories by Numerical Simulation*, Nucl. Phys. B **339**, 222 (1990).
- [9] M. Luscher, *Two particle states on a torus and their relation to the scattering matrix*, Nucl. Phys. B **354**, 531 (1991).
- [10] M. Luscher, *Signatures of unstable particles in finite volume*, Nucl. Phys. B **364** (1991) 237.
- [11] S. Flugge, *Practical Quantum Mechanics*, Springer-Verlag, Berlin (1994), problem n. 27, *Virtual levels*.

- [12] R. G. Winter, “*Evolution of a Quasi-Stationary State,*” Phys. Rev. **123**, n. 4, pag. 1503 (1961).
- [13] U. G. Aglietti and P. M. Santini, “*Analysis of a Quantum Mechanical Model for Unstable Particles*”, arXiv:1010.5926v2 [quant-ph] and references therein.
- [14] U.G. Aglietti and P.M. Santini, “*Renormalization in the Winter Model*”, Phys. Rev. A **89**, 022111 (2014).
- [15] U. G. Aglietti and P. M. Santini, “*Geometry of Winter Model*”, J. Math. Phys. **56** (2015) no.6, 062104, arXiv:1503.02532 [hep-th].
- [16] R. de la Madrid, *The decay widths, the decay constants, and the branching fractions of a resonant state*, Nucl. Phys. A **940** (2015) 297, arXiv:1505.07139 [quant-ph].
- [17] U. G. Aglietti, *1/n-expansion of resonant states*, Mod. Phys. Lett. A **31** (2016) no.25, 1650154, arXiv:1603.02857 [quant-ph].
- [18] R. de la Madrid, “*Numerical calculation of the decay widths, the decay constants, and the decay energy spectra of the resonances of the delta-shell potential*, Nucl. Phys. A **962** (2017) 24, arXiv:1704.00047 [quant-ph], and references therein.
- [19] For a general discussion on  $\delta$ -potentials in quantum mechanics, see: R. Jackiw, *Delta function potentials in two-dimensional and three-dimensional quantum mechanics*, published in “Diverse topics in theoretical and mathematical physics”, 35-53, MIT-CTP-1937.
- [20] See for example: A. H. Nayfeh and D. T. Mook, *Non-linear Oscillations*, WILEY-VCH Verlag GmbH & Co. KGaA, Weinheim (2004).